J|A|C|S ARTICLES

Published on Web 03/04/2010

Continuous Symmetry Breaking Induced by Ion Pairing Effect in Heptamethine Cyanine Dyes: Beyond the Cyanine Limit

Pierre-Antoine Bouit,[†] Christophe Aronica,[†] Loïc Toupet,[‡] Boris Le Guennic,[†] Chantal Andraud,*[,†] and Olivier Maury*[,†]

University of Lyon, Laboratoire de Chimie, UMR 5182 CNRS - Ecole Normale Supérieure de Lyon, 46 allée d'Italie, 69007 Lyon, France, and Institut de Physique - IPR - UMR CNRS 6251, Université de Rennes, 1 Bâtiment 11A, 35042 Rennes Cedex, France

Received December 7, 2009; E-mail: olivier.maury@ens-lyon.fr

Abstract: The association of heptamethine cyanine cation $\mathbf{1}^+$ with various counterions A (A = Br^-, I^-, PF_6^-, SbF_6^-, $B(C_6F_5)_4^-$, TRISPHAT) was realized. The six different ion pairs have been characterized by X-ray diffraction, and their absorption properties were studied in polar (DCM) and apolar (toluene) solvents. A small, hard anion (Br^-) is able to strongly polarize the polymethine chain, resulting in the stabilization of an asymmetric *dipolar-like* structure in the crystal and in nondissociating solvents. On the contrary, in more polar solvents or when it is associated with a bulky soft anion (TRISPHAT or $B(C_6F_5)_4^-$), the same cyanine dye adopts preferentially the *ideal polymethine state.* The solid-state and solution absorption properties of heptamethine dyes are therefore strongly correlated to the nature of the counterion.

Introduction

Since their initial use as sensitizer for silver halide emulsion photography, streptopolymethine dyes (or polymethine dyes)[1] have been continuously studied in the material sciences for numerous applications in optoelectronics, nonlinear optics, optical data storage, organic photovoltaics, or electroluminescence.[2] More recently, they showed promising potentialities in biology as photodynamic therapy agents or bioprobes for near-infrared (NIR) imaging.[3] The main peculiarity of polymethine dyes consists in the odd number of sp^2 carbon atoms forming the π-conjugated bridge between electron-donating and/or -accepting groups, controlling the photophysical and structural properties of the dye. This family can be divided in two subclasses featuring very different structural, electronic and optical properties, depending on the charge of the dye, *i.e.* the neutral (sometimes zwitterionic) *merocyanine* and the charged (cationic or anionic) *cyanine* (Figure 1). The merocyanine subclass can be represented using three different resonance limit structures ($\boldsymbol{M}^{1-3}$) formalized by Dähne in the early 1970s:[4]

(i) The neutral ground state ($\boldsymbol{M}^1$) for weak to moderate electron-donating and -withdrawing groups. This *polyene-like* form is structurally characterized by a maximal bond length alternation[5] (BLA; difference between consecutive single and double bonds) and optically by a broad intense charge transfer transition (CT) featuring positive solvatochromism.

(ii) The zwitterionic case ($\boldsymbol{M}^3$) where complete charge separation occurs under the effect of very strong donor and acceptor fragments. This bipolar polyene structure, also called *betaine*, presents opposite although maximal BLA and a broad CT transition but with a negative solvatochromism.

(iii) Between these two limit structures, for a certain ratio between electron-donating and -accepting characters, the charge of the end-groups equalizes and the BLA vanishes. This particular structure ($\boldsymbol{M}^2$) is called "*cyanine limit*" and is characterized by a sharp, intense absorption band shifted toward the red−NIR spectral range.

In the merocyanine subclass, it is possible to control the neutral or zwitterionic character of the ground state by fine-tuning the strength of the electron-donating/-accepting end-groups or solvent polarity effects (solvatochromism). It is

[†] University of Lyon.
[‡] University of Rennes.

(1) For reviews see: (a) Kulinich, A. V.; Ishchenko, A. A. *Russ. Chem. Rev.* **2009**, *78*, 141–162. (b) Mishra, A.; Behera, R. K.; Behera, P. K.; Mishra, B. K.; Behera, G. B. *Chem. Rev.* **2000**, *100*, 1973–2011. (c) Fabian, J. *Chem. Rev.* **1992**, *92*, 1197–1226.

(2) For selected recent examples see: (a) Bouit, P.-A.; Rauh, D.; Neugebauer, S.; Delgado, J.-L.; Di Piazza, E.; Rigaut, S.; Maury, O.; Andraud, C.; Dyakonov, V.; Martin, N. *Org. Lett.* **2009**, *11*, 4806–4809. (b) Silvestri, F.; Irwin, M. D.; Beverina, L.; Facchetti, A.; Pagani, G. A.; Marks, T. J. *J. Am. Chem. Soc.* **2009**, *130*, 17640–17641. (c) Bouit, P.-A.; Westlund, R.; Feneyrou, P.; Maury, O.; Malkoch, M.; Malmström, E.; Andraud, C. *New J. Chem.* **2009**, *33*, 964–968. (d) Kronenberg, N. M.; Deppish, M.; Würthner, F.; Lademann, H. V. A.; Deing, K; Meerholz, K. *Chem. Commun.* **2008**, *648*, 9–6491. (e) Bouit, P.-A.; Wetzel, G.; Berginc, G.; Toupet, L.; Feneyrou, P.; Bretonnière, Y.; Maury, O.; Andraud, C. *Chem. Mater.* **2007**, *19*, 5325–5335. (f) Hales, J. M.; Zheng, S.; Barlow, S.; Marder, S. R.; Perry, J. *J. Am. Chem. Soc.* **2006**, *128*, 11362–11363.

(3) For selected recent examples see: (a) Kundu, K.; Knight, S. F.; Willett, N.; Lee, S.; Taylor, W. R.; Murthy, N. *Angew. Chem., Int. Ed.* **2009**, *48*, 299–303. (b) Kim, E.-M.; Park, E.-H.; Cheong, S.-J.; Lee, C.-M.; Jeong, H.-J.; Kim, D. W.; Lim, S. T.; Sohn, M.-H. *Bioconjugate Chem.* **2009**, *20*, 1299–1306. (c) Bhushan, K. R.; Misra, P.; Liu, F.; Mathur, S.; Lenkinski, R. E.; Frangioni, J. V. *J. Am. Chem. Soc.* **2008**, *130*, 17648–17649. (d) Li, C.; Greenwood, T. R.; Bhujwalla, Z. M.; Glunde, K. *Org. Lett.* **2006**, *8*, 3623–3626. (e) Zhang, Z.; Achilefu, S. *Chem. Commun.* **2005**, 5887–5889.

(4) Dähne, S.; Radeglia, R. *Tetrahedron* **1971**, *27*, 3673–3696.

(5) The BLA parameter, also called Bonds Order Alternation (BOA) was emphasized by Marder to rationalize empirically the second-order nonlinear optical activity of push−pull dyes. See: (a) Bourhill, G.; Brédas, J. L.; Cheng, L. T.; Marder, S. R.; Meyers, F.; Perry, J. W.; Tiemann, B. G. *J. Am. Chem. Soc.* **1994**, *116*, 2619–2620. (b) Marder, S. R.; Kippelen, B.; Jen, A. K.-Y.; Peyghambarian, N. *Nature* **1997**, *388*, 845–851.

 10.1021/ja9100886

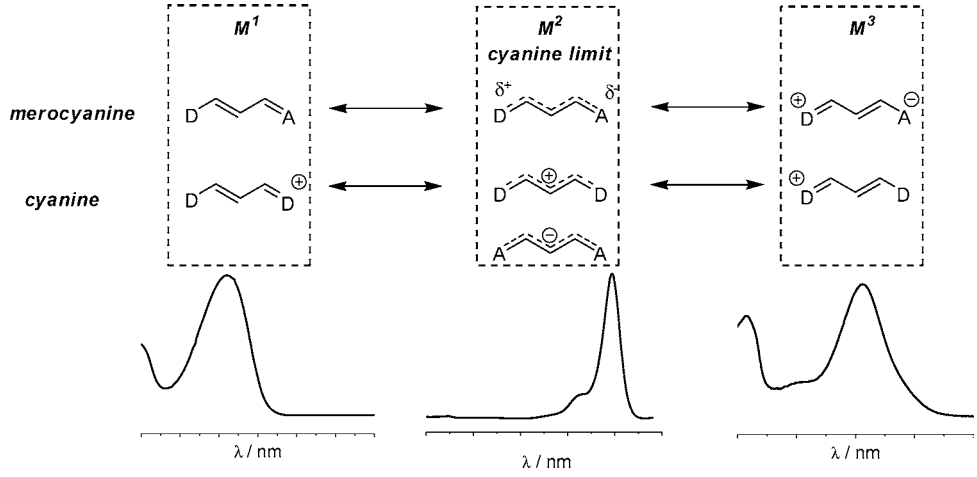

Figure 1. Different resonance forms proposed for push−pull chromophores and related shape of the absorption spectra (bottom).

therefore possible to cross this virtual cyanine limit[6] and, in some rare cases, to stabilize a merocyanine dye close to this ideal cyanine structure.[7]

This cyanine structure, extremely difficult to obtain from dissymmetric merocyanine dyes, can be directly prepared by the association of two identical donor or, more rarely, acceptor end-groups via a polymethine chain featuring an odd number of sp^2 carbon atoms.[8] These molecules spontaneously reach the *ideal polymethine state* (IPS) presenting unique structural and spectral characteristics (Figure 1, M^2). As a result of the two degenerated resonance forms with the charge localized at one or the other end-group ($M^1 = M^3$), the polymethine chain adopts a nonalternating structure with an average "one and a half" bond length (BLA = 0). This lack of bond alternation is experimentally confirmed by most crystal structures reported in the literature.[8a,9] From a spectroscopic point of view, cyanines in their IPS are characterized by a sharp, extremely intense absorption band (Figure 1, M^2) resulting from the reduced vibronic contribution in these nonalternating structures. This particular transition, called solitonic transition by analogy with doped polyacetylene, is shifted toward the NIR spectral range. The complete rationalization of this transition using theoretical models remains a matter of debate; in particular the clear assignment of the high-energy shoulder remains problematic.[10]

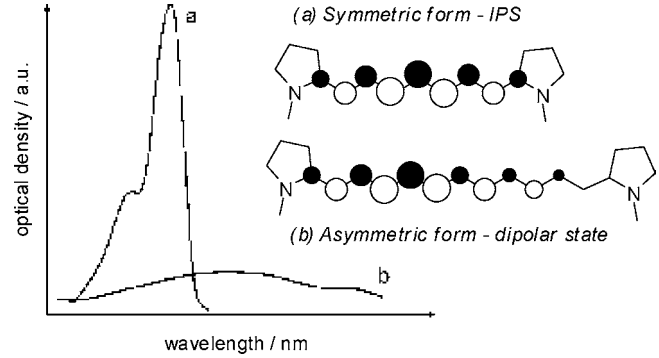

Figure 2. Spectral and electronic modifications by crossing the cyanine limit.[14]

The IPS is conserved in the case of relatively short π-conjugated chains (up to 9−13 carbon atoms, depending on the structure) but is progressively lost for longer chains. As a consequence, upon increasing the chain length, the sharp transition characteristic of the IPS undergoes a bathochromic shift (∼100 nm per additional vinylic unit, Figure 2, curve a) followed by a deep modification of the spectrum with a large broadening of the band and a decrease of its intensity (Figure 2, curve b).[11,12] This chain-length dependence of the spectroscopic properties, generally referred as Brooker experiment,[13] was rationalized first by Tolbert and co-workers[11] invoking a "symmetry collapse" for long-chain cyanine electronic structures due to a Peierls-type distortion. In such a case, the cyanine is no longer symmetric which means it has lost its IPS. Instead it adopts a *dipolar asymmetric form* (Figure 2), that shows a broad CT transition and not the narrow cyanine transition. This symmetry-lowering distortion was recently confirmed by theoretical calculations.[10,14] In addition, Lepkowicz, Hagan, and co-workers reported that, for a given cyanine featuring an 11-carbon atoms

(6) (a) Rettig, W.; Dekhtyar, M. *Chem. Phys.* **2003**, *293*, 75–90. (b) Ishchenko, A. A.; Kulinich, A. V.; Bondarev, S. L; Knyukshto, V. N. *J. Phys. Chem. A* **2007**, *111*, 13629–13627.

(7) (a) Lawrentz, U.; Grahn, W.; Lukaszuk, K.; Klein, C.; Wortmann, R.; Feldner, A.; Scherer, D. *Chem—Eur. J.* **2002**, *8*, 1573–1587. (b) Würthner, F.; Archetti, G.; Schmidt, R.; Kuball, H.-G. *Angew. Chem., Int. Ed.* **2008**, *47*, 4529–4532. (c) Kulinich, A. V.; Derevyanko, N. A; Ishchenko, A. A.; Bondarev, S. L; Knyukshto, V. N. *J. Photochem. Photobiol., A* **2008**, *200*, 106–113.

(8) For several recent examples see: (a) Bouit, P.-A.; Di Piazza, E.; Rigaut, S.; Le Guennic, B.; Aronica, C.; Toupet, L.; Andraud, C.; Maury, O. *Org. Lett.* **2008**, *10*, 4159–4162. (b) Chen, X.; Peng, X.; Cui, A.; Wang, B.; Wang, L.; Zhang, R. *J. Photochem. Photobiol., A* **2006**, *181*, 79–85. (c) Asato, A. E.; Watanabe, D. T.; Liu, R. S. H. *Org. Lett.* **2000**, *2*, 2559–2562. (d) Peng, X.; Song, F.; Lu, E.; Wang, Y.; Zhou, W.; Fan, J; Gao, Y *J. Am. Chem. Soc.* **2005**, *127*, 4170–4171.

(9) (a) Yau, C. M. S.; Pascu, S. I.; Odom, S. A.; Warren, J. E.; Koltz, E. J. F.; Frampton, M. J.; Williams, C. C.; Coropceanu, V.; Kuimova, M. K.; Phillips, D.; Barlow, S.; Brédas, J.-L.; Marder, S. R.; Millar, V.; Anderson, H. L. *Chem. Commun.* **2008**, 2897–2899. (b) Nagao, Y.; Sakai, T.; Kozawa, K.; Urano, T. *Dyes Pigm.* **2007**, *73*, 344–352. (c) Dai, Z. F.; Peng, B. X.; Chen, X. A. *Dyes Pigm.* **1999**, *40*, 219–223. (d) Koska, N. A.; Wilson, S. R.; Schuster, G. B. *J. Am. Chem. Soc.* **1993**, *115*, 11628–11629. (e) Kulpe, S.; Kuban, R. J.; Schulz, B.; Dähne, S. *Cryst. Res. Technol.* **1987**, *22*, 375–379.

(10) (a) Egorov, V. V. *J. Chem. Phys.* **2002**, *116*, 3090–3102. (b) Kachkovsky, O. D.; Shut, D. M. *Dyes Pigm.* **2006**, *71*, 19–27. (c) Guillaume, M.; Liégeois, V.; Champagne, B.; Zutterman, F. *Chem. Phys. Lett.* **2007**, *446*, 165–169.

(11) Tolbert, L. M.; Zhao, X. *J. Am. Chem. Soc.* **1997**, *119*, 3253–3258.

(12) Kachkovski, O. D.; Tolmachov, O. I.; Slominskii, Y. L.; Kudinova, M. O.; Derevyanko, N. O.; Zhukova, O. O. *Dyes Pigm.* **2005**, *64*, 207–216.

(13) Brooker, L. G. S.; Sprague, R. H; Smyth, C. P.; Lewis, G. L. *J. Am. Chem. Soc.* **1940**, *62*, 1116–1125.

(14) Fabian, J. *J. Mol. Struct. (THEOCHEM)* **2006**, *766*, 49–60.

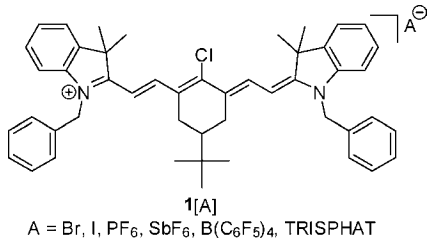

Figure 3. Molecular structure of the cyanine cation and associated anions.

conjugated chain, it is possible to cross the "*cyanine limit*" by increasing the solvent polarity.[15] The observed positive solvatochromism, characteristic of push−pull dyes featuring a large ground-state dipole moment, allowed the authors to conclude that a "polymethine chain may exist in the ground state in two charged forms with *symmetrical* and *asymmetrical* distribution of charge density" (Figure 2). The existence of the asymmetric form was further evidenced by X-ray crystallography in the case of a particular trimethynecyanine $[Mc(CH_2)_3Mc]^+$ featuring ruthenocenyl donor (Mc) end group.[16] This result is quite surprising because the cyanine bridge is very short, which generally favors the symmetric form, and because the ferrocenyl analogously remains symmetric. The authors explain these distortions by electronic effects rather than solid-state crystal packing effects.

In summary, it has been demonstrated to date that the cyanine limit can be crossed (i) by the modification of the donor end-group, (ii) by lengthening of the conjugated skeleton, or (iii) by increasing the solvent polarity for a given cyanine. It is worth noting that the influence of the counterion on the properties of cationic cyanine dyes was neglected among the large literature devoted to this class of chromophores. However, one can mention the works of Schuster and co-workers in the 1990s, who reported the induction of circular dichroism by interaction between cyanine salts and chiral borate anions[17] and that of Heier and co-workers on the nanostructure and conducting properties of fullerene−cyanine blends with different counterions.[18] In this context, we recently described the diastereoselective supramolecular interaction between a TRISPHAT anion and the heptamethine cyanine $\mathbf{1}^+$ (Figure 3).[19]

In the present article, we present a combined crystallographic−spectroscopic study of the influence of the counterion A (A = Br^-, I^-, PF_6^-, SbF_6^-, $B(C_6F_5)_4^-$, TRISPHAT) on the solution and solid-state properties of the **1**·[A] cyanine salt (Figure 3). Whereas the ideal polymethine state is maintained in the case of large counterions, under some particular conditions, the formation of an ion-pair with a small counterion will favor the unsymmetrical form.

Results and Discussion

Synthesis. 1·[Br] was synthesized using classical procedures[2e] and used as starting material for all anion-exchange reactions.

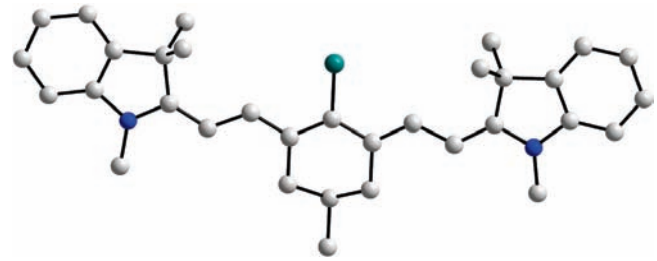

Figure 4. DFT optimized structure of $\mathbf{1'}^+$. In the ball-and-stick representation, carbon, nitrogen, and chloride atoms are colored in gray, blue, and green, respectively. H atoms were omitted for clarity.

Table 1. C−C Bond Lengths (in pm) Determined by DFT Calculations or by Crystallography

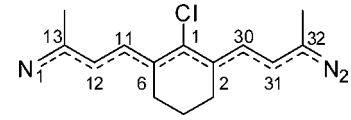

	1·[Br]	**1**·[I]	**1**·[PF_6]	**1**·[SbF_6]	**1**·[$B(C_6F_5)_4$]	**1**·[TRISPHAT]	$\mathbf{1'}^{+\,d}$
C13−C12	141.2	139.4	138.1	140.9	139.3	139.1	139.6
C12−C11	136.0	139.4	137.5	137.0	136.4	139.1	140.0
C11−C6	140.5	140.0	139.5	140.6	140.3	139.0	140.1
C6−C1	137.1	139.5	138.0	138.4	139.5	140.2	141.2
C1−C2	142.3	143.8	141.0	142.3	139.9	140.7	141.2
C2−C30	135.9	137.2	138.7	139.5	139.2	138.6	140.1
C30−C31	142.4	140.8	139.7	139.6	138.7	139.8	140.0
C31−C32	134.8	136.7	136.8	138.5	138.3	137.5	139.6
l_1[a]	141.6	141.0	139.6	140.8	139.5	−[c]	−[c]
l_2[b]	135.9	138.2	137.8	138.3	138.3	−[c]	−[c]
BLA	5.7	2.8	1.8	2.5	1.2	−[c]	−[c]

[a] Average of the short bond lengths [b] Average of the long bond lengths. [c] Not possible to determine. [d] DFT optimized structure.

The displacement of the bromide anion required an excess of NaI, $NaPF_6$, and $NaSbF_6$, but only one equivalent of the more lipophilic $[HNBu_3][TRISPHAT]$ or $[Li][B(C_6F_5)_4]\cdot Et_2O$ salts. All the products **1**·[Br], **1**·[I], **1**·PF_6], **1**·[SbF_6], **1**·[TRISPHAT], and **1**·[$B(C_6F_5)_4$] were purified by extraction, filtration on a silica plug, and crystallization from toluene−chloroform or toluene−methanol mixtures (see Experimental Section). The resulting single crystals all display a metallic shine and were further used for crystallography or spectroscopy experiments.

Gas-Phase Structure. The gas-phase structure of the cation $\mathbf{1'}^+$, without a counterion and featuring N−Me instead of N−Bn moieties, was obtained using density functional theory calculations (DFT, see Experimental Section for computational details). The optimized structure of the *syn* conformation with both NMe groups opposite to Cl has been calculated to be 3.3 kcal·mol^{-1} more stable than the structure with both NMe on the same side as Cl in agreement with the structure obtained by X-ray crystallography (vide infra). The structure is perfectly planar without any twist of the carbon skeleton. All C−C bond lengths of the polymethine backbone are similar (140.2 ± 1 pm). This value is intermediate between single and double bonds (Table 1), and this perfectly nonalternating structure is characteristic of the IPS.

Solid-State Structures. The X-ray diffraction analysis of the six cyanine salt crystals was performed. Crystal data and refinement parameters are summarized in Table 3 (see Experimental Section for details). For clarity, the same atom numbering is used for the cyanine cation in each structure (Table 1). At the molecular level the cyanine cation always presents the expected *syn* conformation with both N−Bn moieties located

(15) Lepkowicz, R. S.; Przhonska, O. V.; Hales, J. M.; Fu, J.; Hagan, D. J.; Van Stryland, E. W.; Bondar, M. V.; Slominsky, Y. L; Kachkovski, A. D. *Chem. Phys.* **2004**, *305*, 259–270.
(16) Barlow, S.; Henling, L. M.; Day, M. W.; Marder, S. R. *Chem. Commun.* **1999**, 1567–1568.
(17) (a) Owen, D. J.; Schuster, G. B. *J. Am. Chem. Soc.* **1996**, *188*, 259–256. (b) Owen, D. J.; Van Derveer, D.; Schuster, G. B. *J. Am. Chem. Soc.* **1998**, *120*, 1705–1717.
(18) Heier, J.; Groenewold, J.; Huber, S.; Nüesch, F.; Hany, R. *Langmuir* **2008**, *24*, 7316–7322.
(19) Bouit, P.-A.; Aronica, C.; Guy, L.; Martinez, A.; Andraud, C.; Maury, O. *Org. Biomol. Chem.* **2009**, *7*, 3086–3090.

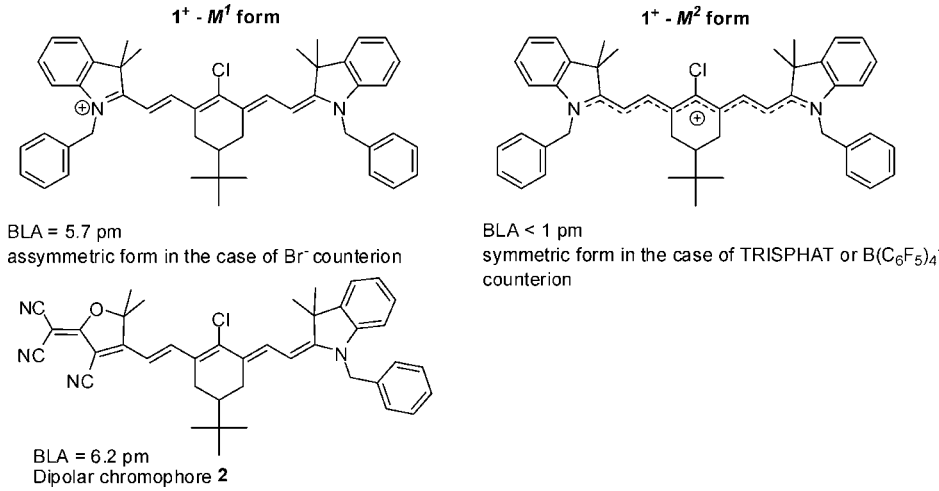

Figure 5. Different structures observed for the cyanine cation $\mathbf{1}^+$. The chromophore **2** is shown for comparison.

at the opposite side of the chlorine atom. The π-conjugated skeleton is quasi-planar with a small overall tilt angle (dihedral angle N1−C13−C32−N2) lying between 8.6 and 30°. The planarity of the conjugated carbon chain is ensured by the fused, central 6-membered ring whose conformation is further constrained by the thermodynamically favored equatorial position of the *tert*-butyl fragment. The most striking difference observed between the six cyanine salts concerns the C−C bond distances in the conjugated backbone and, more precisely, in the overall BLA defined here as the difference between the average of the short and the long C−C bond lengths (Table 1). The **1**·[TRISPHAT] salt presents an almost perfectly nonalternated structure, where it is not possible to discriminate between short and long C−C bond lengths. In this case, the BLA is almost zero as expected for a cyanine in its IPS. The structure of the **1**·[Br] salt is in marked contrast with the previous one since a clear alternation between short (135.9 pm) and long (141.6 pm) C−C bonds is observed, leading to a large BLA value of 5.7 pm. This result indicates a significant breaking of the molecular symmetry which is further confirmed by the analysis of the terminal C−N distances. With 133.6 pm, the N1−C13 bond length is in the range of an imine/iminium fragment, while the N2−C32 bond measures 140.9 pm which is closer to the length of an amine moiety. In the **1**·[Br] salt, the cyanine cation loses its IPS state, the molecule being polarized with one amino- and one iminium-like moiety at each extremity bridged by an alternating π-conjugated backbone. **1**·[Br] presents a close structural similarity with the previously described dipolar compound **2** in which a tricyanofurane accepting group is associated with an amino donor group via the same conjugated bridge and which exhibits a BLA value of 6.2 pm (Figure 5).[2e] To the best of our knowledge, **1**·[Br] is until now the only heptamethine structure featuring such a marked dipolar character.[20] The structures of the four other salts are intermediate between the two limits, *i.e.* IPS and dipolar form. The BLA depends strongly on the nature of the counterion and decreases in the series $Br^- \gg I^- \approx SbF_6^- > PF_6^- > B(C_6F_5)_4^- >$ TRISPHAT (Table 1). To get a deeper insight into these solid-state effects, a careful examination of the crystal packing was undertaken.

In spite of their large BLA difference, **1**·[Br] and **1**·[I] are isostructural and crystallized in the $P2_1/c$ space group. The crystal lattice is made of zigzag double layers of stacked cations separated by sheets of halogenide anions (Figure 6, up). Each cation is surrounded by seven nearest anions within a radius of 10 Å. Whereas N1 is close to three halogenides (d(N1−Br) = 4.74, 4.86, and 6.95 Å; d(N1−I) = 4.86, 5.01, and 6.88 Å), N2 has four anionic neighbors (d(N2−Br) = 6.91, 7.04, 8.18, and 8.55 Å; d(N2−I) = 6.91, 7.02, 8.10, and 8.56 Å) (Figure 6, bottom). Therefore, from a pure structural point of view, in the case of **1**·[Br] and **1**·[I], the anionic environment of the cyanine is clearly unsymmetrical and can probably account for the polarization of the polymethine chain, the nitrogen atom with an iminium character being located in the closest anionic neighborhood. However, this crystallographic description is insufficient to explain the difference in the magnitude of the BLA observed for these two compounds (Table 1). The nature of the anion has to be taken into account, too. Indeed, according to the HSAB theory (Pearson's hard and soft acid−base theory), a stronger polarization is expected upon interaction with a hard counterion. In the present case, bromide featuring the same charge but a smaller ionic radius than iodide can be considered as the harder anion. As a consequence, for a given interaction

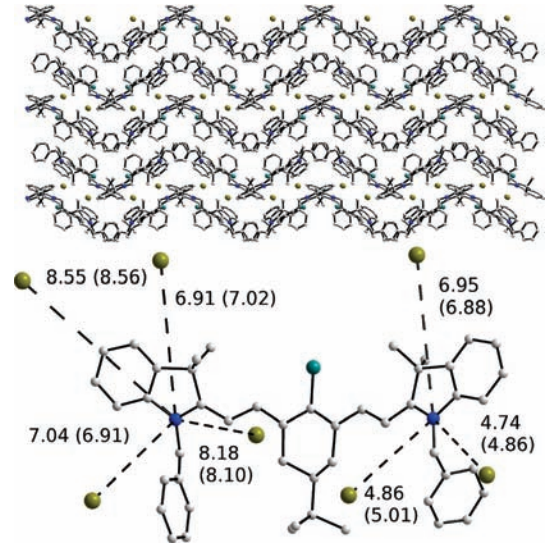

Figure 6. View of the crystal packing of **1**·[Br] according to the c axis (up). Position and distances (in Å) of nearest anionic environment of the cyanine cation in the cases of **1**·[Br] (**1**·[I] in parentheses, bottom).

(20) The alternating cyanine described in ref 16 presents a BLA of 10 pm but possesses a conjugated chain composed of only three carbon atoms.

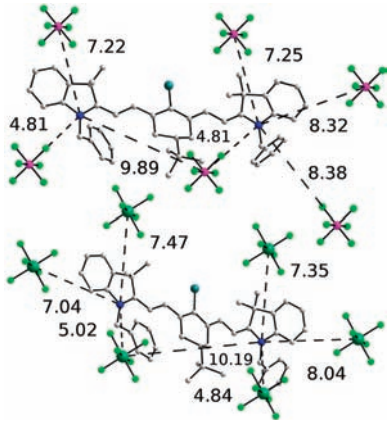

Figure 7. Position and distances (in Å) of nearest anionic environment of the cyanine cation in the case of **1**·[PF_6] (up) and **1**·[SbF_6] (bottom).

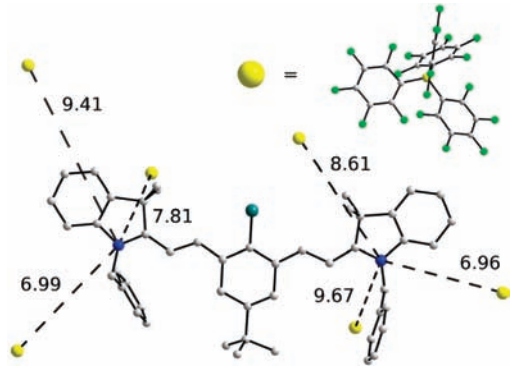

Figure 8. Position and distances (in Å) of nearest anionic environment of the cyanine cation in the case of **1**·[$B(C_6F_5)_4$].

(same distance, same anionic surrounding) bromide polarizes the polymethine chain more strongly than iodide.

1·[PF_6] and **1**·[SbF_6] also form a pair of isostructural compounds crystallizing in the centrosymmetric $P\bar{1}$ space group. The crystal lattice is constituted of parallel double-layers of cations separated by a single sheet of counterions (Figure 7, up). In these structures, the anionic surrounding is composed of six anions, from which one is in interaction with both sides of the cyanine. Two shorter anion−cation distances, responsible for the stronger electrostatic interaction, are observed on both sides of the molecule (d(N1−P) = d(N2−P) = 4.81 Å and d(N1−Sb) = 5.02 and d(N2−Sb) = 4.84 Å), the other anions being located far away, at a distance higher than 7 Å (Figure 7). A fairly symmetric anion environment is also formed for the **1**·[$B(C_6F_5)_4$] crystal structure (triclinic, $P\bar{1}$ space group) where the cation interacts with six borate anions (Figure 8) located at larger distances due to the large steric hindrance induced by this bulky anion (d(N1−B) = 6.99, 7.81, 9.41 Å and d(N2−B) = 6.96, 8.61, 9.67 Å). In the latter three cases, the anion-surrounding of the cyanine cation is clearly more symmetrical than in **1**·[Br] and **1**·[I]. Whatever the nature of the anions, this symmetric environment results in a very small polarization of the polymethine chain compared to that of **1**·[Br]. Finally, in the case of **1**·[TRISPHAT], a diastereoselective supramolecular interaction occurs between the TRISPHAT anion and the *pro*-chiral cyanine anion.[19] As a result, the cation presents a close interaction with one anion (d(N1−P) = 5.22 Å) and long distance ones with four other anions (Figure 9). In spite of this unsymmetrical environment, the polymethine chain shows no sign of polarization (BLA = 0, Table 1). The

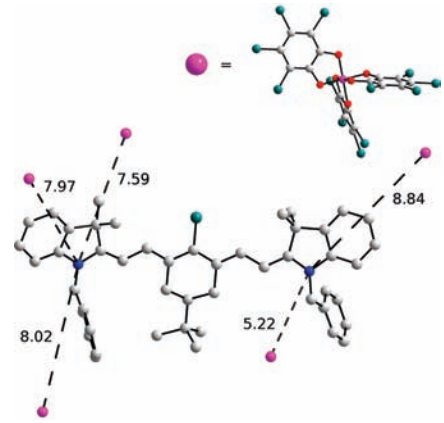

Figure 9. Position and distances (in Å) of nearest anionic environment of the cyanine cation in the case of **1**·[TRISPHAT].

TRISPHAT anion is bulky, and the negative charge is delocalized over the three tetrachlorophenyl accepting moieties. It can therefore be considered as a soft anion, unable to induce any electronic polarization.

As a summary of this first part, it is noticeable that a given cyanine cation can generate different structures in the solid state, depending on the nature of the associated counterion and on the symmetry of the anionic surrounding. A relatively small, hard anion in a nonsymmetric environment is able to strongly polarize the polymethine chain, resulting in a BLA comparable to that of related dipolar molecules. On the other hand, a softer anion does not polarize significantly the conjugated chain whatever the symmetry of the packing. The same cyanine cation can therefore present two different structures in the solid state: a classical *nonalternating IPS* and a very scarce *dipolar* one. This unambiguously demonstrates that the electronic structure of the polymethine chain in the crystal may be controlled by anion/cation interactions.

Absorption Spectroscopy. The electrostatic interactions between anions and cations can also be controlled in solution by tuning the solvent polarity: whereas polar solvents lead to the formation of dissociated solvated anions and cations, apolar solvents favor associated ion-pairs. Therefore, the absorption properties of the different salts have been studied both in a nondissociating solvent like toluene featuring a very low dielectric constant (ε_r = 1) and in a more polar one, dichloromethane (DCM, ε_r = 9).

In DCM, all cyanine salts present a very similar spectrum with a sharp absorption band at 794 nm with giant extinction coefficients (300−350 000 L·mol^{-1}·cm^{-1}, the variations being within the experimental error) characteristic of a cyanine salt in its IPS (Figure 10 and Table 2, note that the rising feature around 900 nm is due to baseline problem at the upper detection limit). In such a relatively polar solvent the cyanine salts are dissociated, and therefore the counterions do not play any role in the absorption properties. In the absence of counterions, the cyanine cation presents the classical IPS as illustrated by the calculation for the free ion.

On the contrary, the different cyanine salts present completely different absorption spectra in toluene (Figure 11, up). Cyanine salts featuring bulky counterion like **1**·[$B(C_6F_5)_4$] or **1**·[TRISPHAT] show a similar spectrum as in DCM indicating that the cyanine remains in the IPS. In marked contrast, for **1**·[Br] the sharp transition observed in DCM completely collapses in toluene (ε = 72 000 L·mol^{-1}·cm^{-1}) whereas the

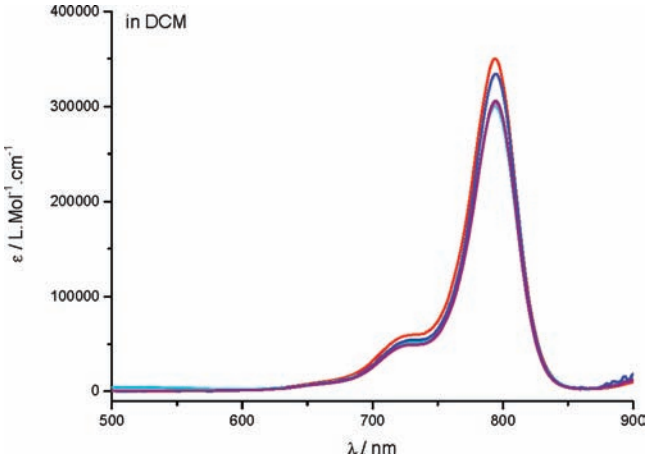

Figure 10. Absorption spectra of compounds **1**·[TRISPHAT] (purple), **1**·[$B(C_6F_5)_4$] (blue), **1**·[PF_6] (cyan), **1**·[SbF_6] (magenta), **1**·[I] (orange) and **1**·[Br] (red) in DCM.

Table 2. Photophysical Data of **1**·**[A]** in DCM and Toluene

	DCM		toluene	
compound	λ_{max} (nm)	ε (L·mol^{-1}·cm^{-1})	λ_{max} (nm)	ε (L·mol^{-1}·cm^{-1})
1·[Br]	794	350 000	761	72 000
1·[PF_6]	794	300 000	779	117 000
1·[I]	794	305 000	782	110 000
1·[SbF_6]	794	305 000	776	117 000
1·[$B(C_4F_5)_4$]	794	330 000	799	268 000
1·[TRISPHAT]	794	320 000	792	310 000

higher energy shoulder seems to be less affected by the solvent modification. This profound change in the absorption spectrum is continuous as illustrated by the series of spectra recorded in various dichloromethane-toluene mixtures (Figure 11, bottom). Importantly, the final spectrum of **1**·[Br] in toluene presents strong similarities with the spectrum of the neutral dipolar compound **2** recorded in DCM (Figure 11, bottom), suggesting that, in toluene, **1**·[Br] exists in a *dipolar* form (Figure 5). This symmetry collapse is probably due to the formation of an asymmetric ion-pair between $\mathbf{1}^+$ and Br^- resulting in the polarization of the polymethine chain in agreement with the solid state structure featuring a large BLA (*vide supra*). The continuous transition from the IPS observed in DCM to the dipolar state observed in toluene is simply driven by the thermodynamic solvation equilibrium between dissociated and associated ion pairs.

The absorption spectra in toluene of the other cyanine salts (**1**·[I], **1**·[PF_6], and **1**·[SbF_6]) are intermediate between those of **1**·[Br] and **1**·[$B(C_6F_5)_4$] (or **1**·[TRISPHAT]). The sharp transition characteristic of IPS cyanine remains visible but is significantly attenuated with extinction coefficients around 110−120000 L·mol^{-1}·cm^{-1}. This result can be interpreted in two ways: (i) the thermodynamic solvation equilibrium is not fully displaced in favor of the associated or dissociated species, the two limit forms being present in solution in different amounts depending on the nature of the counterion. In such a case, the experimental absorption spectrum results from their relative contributions. (ii) A single species is present in solution with its own absorption spectrum, but the polarization of the polymethine chain, controlled by the interaction with the counterion is intermediate between the two limit forms.

Our experimental results are in line with the interpretation proposed by Lepkowicz, Hagan, and co-workers.[15] These authors proposed that the cyanine cation should be present in its ground state in two different forms with *symmetrical* and *asymmetrical* distribution of the charge density separated by an energy barrier. In the light of the above-mentioned results,

Table 3. Crystal Data and Structure Refinement Parameters

	1·[Br]	**1**·[I]	**1**·[$B(C_6F_5)_4$]	**1**·[PF_6]	**1**·[SbF_6]
formula	$C_{48}H_{52}BrClN_2$	$C_{48}H_{52}ClIN_2$	$C_{72.50}H_{54}BClF_{20}N_4O_{0.50}$	$C_{58.50}H_{64}ClF_6N_2P$	$C_{55}H_{60}ClF_6N_2Sb$
fw (g·mol^{-1})	772.28	819.27	1415.46	975.54	1020.25
cryst. syst.	monoclinic	monoclinic	triclinic	triclinic	triclinic
space group	$P2_1/c$ (No. 14)	$P2_1/c$ (No. 14)	$P\bar{1}$ (No. 2)	$P\bar{1}$ (No. 2)	$P\bar{1}$ (No. 2)
a (Å)	12.676 (7)	12.473 (1)	13.237 (7)	9.665 (7)	10.023 (6)
b (Å)	19.587 (9)	19.634 (1)	14.661 (8)	14.125 (1)	15.406 (9)
c (Å)	17.606 (8)	17.670 (1)	17.009 (8)	20.717 (1)	18.064 (9)
α (deg)	90.0	90.0	84.837 (4)	75.156 (6)	67.377 (6)
β (deg)	103.143 (5)	103.098 (3)	85.032 (4)	87.153 (6)	83.711 (5)
γ (deg)	90.0	90.0	81.250 (5)	69.688 (7)	77.485 (5)
V (Å^3)	4256.7 (4)	4214.9 (3)	3240.3 (3)	2561.4 (3)	2512.4 (2)
Z	4	4	2	2	2
T (K)	295	110	110	110	110
λ (Mo Kα) (Å)	0.71069	0.71069	0.71069	0.71069	0.71069
D (g·cm^{-3})	1.205	1.291	1.451	1.265	1.349
μ (μm^{-1})	1.06	0.86	0.17	0.17	0.66
$R(F)^a$, $I > 1\sigma(F_o)$	0.073	0.061	0.064	0.051	0.058
$R_w(F^2)^b$, $I > 1\sigma(F_o)$	0.279	0.176	0.193	0.131	0.170
S	0.67	0.80	0.86	0.65	0.77
R_{int}	0.056	0.069	0.032	0.057	0.035
θ_{max}	28.0°	27.0°	32.2°	32.0°	32.0°
h	−16 → 15	−15 → 15	−19 → 15	−6 → 14	−6 → 14
k	−22 → 25	−25 → 25	−17 → 21	−20 → 20	−22 → 22
l	−23 → 23	−22 → 16	−25 → 23	−29 → 30	−26 → 26
parameters	451	469	878	640	614
measured reflections	27204	29286	26729	21313	21602
independent reflections	9784	9147	16798	13603	13897
reflections with $I > 2.0\sigma(I)$	2471	3197	6413	3781	6659
$\Delta\rho_{min}$	−0.33 e Å^{-1}	−0.96	−0.51	−0.29 e Å^{-1}	−1.05 e Å^{-1}
$\Delta\rho_{max}$	0.91 e Å^{-1}	1.23	0.85	0.38 e Å^{-1}	1.17 e Å^{-1}

^{a} $R(F) = \Sigma||F_o|-|F_c||/\Sigma|F_o|$. ^{b} $R_w(F) = \Sigma[w((F_o^2 - F_c^2)^2/\Sigma wF_o^4]^{1/2}$

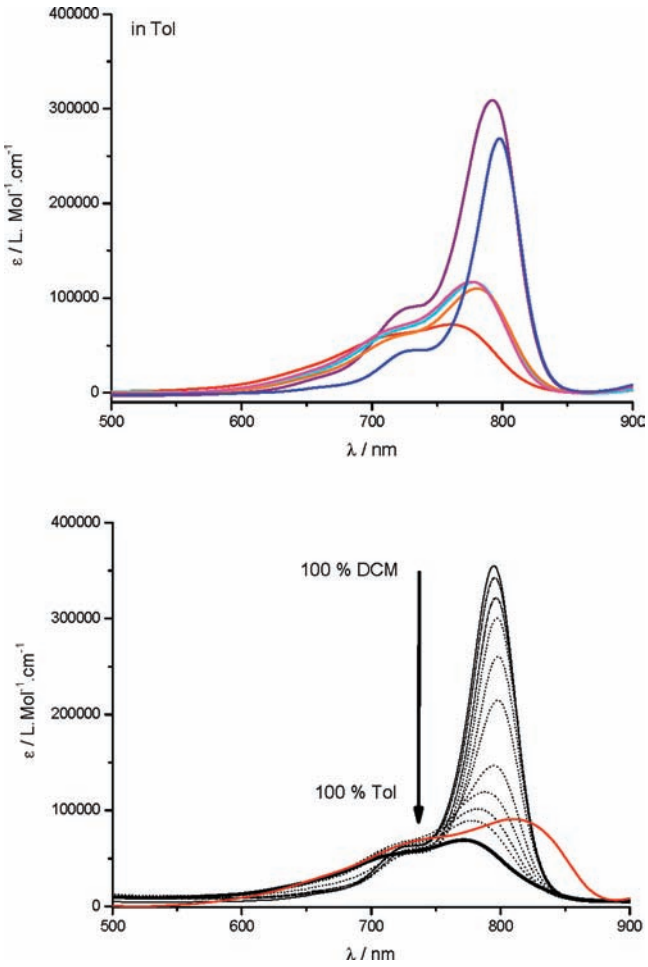

Figure 11. Absorption spectra of compounds **1**·[TRISPHAT] (purple), **1**·[$B(C_6F_5)_4$] (blue), **1**·[PF_6] (cyan), **1**·[SbF_6] (magenta), **1**·[I] (orange), and **1**·[Br] (red) in toluene (up). The bottom figure describes the evolution of the absorption spectrum of **1**·[Br] in DCM/toluene solvent mixtures, (thin) 100/0; (dotted) 90/10, 80/20, 70/30, 60/40, 50/50, 40/60, 30/70, 20/80, 10/90; (bold) 0/100. For comparison, the absorption spectrum of the dipolar compound **2** (red) in DCM is superimposed (bottom).

we proposed another description that takes into account chemical concepts such as ion-pair solvation equilibrium and HSAB theory, often neglected by the spectroscopist community. Such interpretation concerns cyanine featuring relatively short π-conjugated chain length (9−13 C atoms) able to reach their IPS. In this case, the anion-cyanine couple exists in solution in two different forms: (i) an intimate ion pair or (ii) a dissociated ion-pair in a more polar solvent. The dissociated ion-pair presents always the structural and electronic properties of the cyanine cation in its IPS whatever the nature of the anion. In the case of an associated ion-pair two cases must be considered. If the counterion is soft according to the HSAB classification, the cyanine will conserve its IPS structure. On the contrary, a hard anion will localize the positive charge on one side of the polymethine chain resulting in the formation of asymmetrical dipolar structures featuring very different absorption properties.

Consequently, these results are of considerable importance in the field of material science where cyanine dyes are widely used as dopant in polymer or sol−gel matrices developed for photovoltaic or nonlinear optical applications.[2a,f] Depending on the nature of the counterion, the cyanine cation can be present either in its IPS or in a dipolar state which strongly modified its electronic properties. This phenomena is illustrated in the

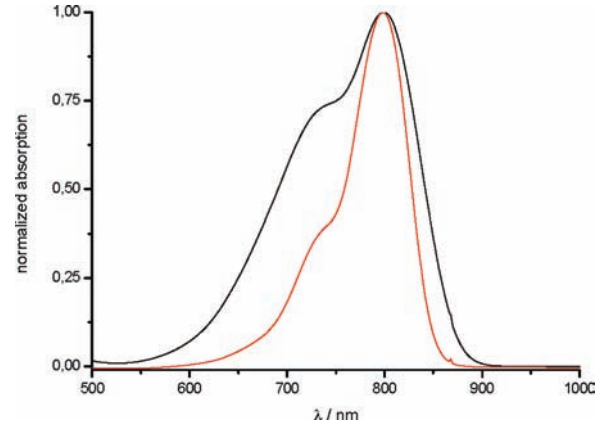

Figure 12. Normalized absorption spectra of PMMA thin films doped with **1**·[Br] (black) and **1**·[TRISPHAT] (red).

Figure 12 which shows the absorption spectra of two polymethylmethachrylate thin films spin coated on glass plates and doped with 10% weight of **1**·[Br] and **1**·[TRISPHAT]. The shapes of the normalized spectra are very different; in particular, the sharp transition of a cyanine in its ideal polymethine states is conserved in the case of the TRISPHAT salt but almost completely disappears for the bromide one. In such materials, the electronic structure of the cyanine cation can therefore be controlled by the interactions with its counterion as already observed in the crystal and in solution.

Conclusion

In this article, we emphasized the tremendous role of the counterion on the structural and electronic properties of a heptamethine cyanine cation. We unambiguously demonstrated that a small, hard anion (bromide) is able to strongly polarize the polymethine chain resulting in the stabilization of an asymmetric *dipolar-like* structure in the crystal and in nondissociating solvent. On the contrary, in more polar solvents or when it is associated with a bulky soft anion (TRISPHAT or $B(C_6F_5)_4^-$), the same cyanine dye preferentially adopts the *ideal polymethine state.* To the best of our knowledge, this is the first time that the same cyanine structure is observed in its two limit forms, a symmetric and a dipolar one, both in solution and in the solid state, simply by tuning the counterion or the solvent polarity. This result is important from a fundamental point of view, since the role of the counterion, which was neglected up to now, can contribute to the explanation of many absorption property modifications induced by the solvent or by interactions with exogenous molecules, even biomacromolecules. In addition, we demonstrated that the nature of the counterion is also able to control the absorption spectrum of a cyanine cation used as dopant in a polymer matrix. In conclusion, the modulation of the structural and electronic properties of cyanine cations by interaction with the counterion is a general phenomenon observed in the crystal, in solution and in a polymeric matrix. In the future, counterion effects have to be considered as important parameters for the design of new cyanine dyes or new cyanine-based applications.

Experimental Section

General. All reactions were systematically performed under argon. NMR spectra (^1H, ^{13}C) were recorded at room temperature on a BRUKER AC 200 operating at 200.13 MHz and 50.32 for ^1H and ^{13}C respectively. Data are listed in parts per million (ppm) and are reported relative to tetramethylsilane (^1H, ^{13}C), residual solvent

peaks being used as internal standard ($CHCl_3$ ^1H: 7.26 ppm, ^{13}C: 77.36 ppm). UV−visible spectra were recorded on a Jasco V-550 spectrophotometer in diluted solution (*ca.* 10^{-5} mol.L^{-1}). High resolution mass spectrometry measurements and elemental analysis were performed at the Service Central d'Analayse du CNRS (Vernaison, France). Column Chromatography was performed on Merck Gerduran 60 (40−63 μm) silica. The synthesis of **1**·[Br][2e] and **1**·[D-TRISPHAT][19] have been reported elsewhere.

Computational Details. The DFT geometry optimization of $\mathbf{1}^+$ was carried out with the Gaussian03 (Revision B.04) package[21] employing the three-parameter hybrid functional of Becke based on the correlation functional of Lee, Yang, and Parr (B3LYP).[22,23] The 6-31G* basis sets were used for C, N, and H atoms, whereas a diffuse function was added for Cl.

X-ray Crystallography. Data Collection. For compounds **1**·[Br], **1**·[I], **1**·[$B(C_6F_5)_4$], **1**·[PF_6], **1**·[SbF_6], processing of the data was performed by the Oxford Diffraction Xcalibur Saphir 3 diffractometer analysis softwares (Crysalis, 2004). The lattice constants were refined by least-squares refinement using 2471 reflections ($2.7° < \theta < 32°$); 3197 ($2.6° < \theta < 27°$), 6413 ($2.6° < \theta < 32°$), 3781 ($2.8° < \theta < 32°$), 6655 ($2.7° < \theta < 32°$) respectively. No absorption correction was applied to data sets.

Structure Solution and Refinement. **1**·[$B(C_6F_5)_4$], **1**·[PF_6], **1**·[SbF_6], crystallize in the triclinic system and according to the observed systematic extinctions, the structures have been solved in the *P-1* space group (No. 2). **1**·[Br], **1**·[I], crystallize in the monoclinic system and according to the observed systematic extinctions, the structures have been solved in the $P2_1/c$ space group (No. 14). The structure was solved by direct methods using the SIR97 program[24] combined to Fourier difference syntheses and refined against *F* square using reflections with $[I/\sigma(I) > 2]$ with SHELXL97.[25] All atomic displacements parameters for non-hydrogen atoms have been refined with anisotropic terms. After anisotropic refinement, all the hydrogen atoms are found with a Fourier Difference. Table 2 summarizes the crystallographic data and refinement parameters for **1**·[Br], **1**·[I], **1**·[$B(C_6F_5)_4$], **1**·[PF_6], **1**·[SbF_6] whose crystal structures have been deposited at the Cambridge Crystallographic Data Centre and allocated to the following deposit numbers, CCDC 620268, CCDC 647547, CCDC 681120, CCDC 634859, and CCDC 668666, respectively.

1·[PF_6] (Method A). **1**·[Br] (1 equiv) is dissolved in the minimal amount of methanol. This solution is added dropwise to an aqueous solution of sodium hexafluorophosphate (50 equiv) under vigorous stirring. The resulting precipitate is filtered, the crude product is dissolved in DCM, the solution is extracted with water (3 × 15 mL) and filtered trough a silica plug (washed with DCM). Then the solvents are evaporated to afford a green solid (86 mg, 80%). Single crystals suitable for X-rays diffraction analysis are obtained by slow evaporation of chloroform-toluene mixture. ^1H NMR (200.13 MHz, $CDCl_3$): δ 0.95 (s, 9H), 1.4 (m, 1H), 1.72 (s, 6H), 1.74 (s, 6H), 2.00 (dd, ^3J = 13 Hz, ^2J = 13 Hz, 2H), 2.57 (dd, ^3J = 2 Hz, ^2J = 13 Hz, 2H), 5.28 (s, 4H), 6.07 (d, ^3J = 14 Hz, 2H), 7.2−7.5 (m, 18H), 8.23 (d, ^3J = 14 Hz, 2H).^{13}C NMR (50.32 MHz, $CDCl_3$): δ 27.3, 28.1, 28.2, 32.3, 42.0, 48.1, 49.3, 102.2, 110.9, 122.5, 125.6, 126.6, 128.4, 129.0, 129.2, 134.2, 140.9, 142.8, 144.4, 150.8, 172.6. ^{31}P NMR (81 MHz, $CDCl_3$): δ 174.2. Anal. Calcd for $C_{48}H_{52}N_2ClF_6P·H_20$: C, 67.40, H, 6.36, N, 3.27, Found C, 67.77, H, 6.32, N, 3.20. UV−vis (CH_2Cl_2): λ_{max} = 794 nm (ε_{max} = 29 0000 L·mol^{-1}·cm^{-1}).

1·[SbF_6]. is synthesized using Method A from **1**·[Br] with [Na][SbF_6]. Single crystals suitable for X-ray diffraction analysis were obtained by slow evaporation of chloroform−toluene mixture. ^1H NMR (200.13 MHz, $CDCl_3$): δ 0.95 (s, 9H), 1.40 (m, 1H), 1.72 (s, 6H), 1.74 (s, 6H), 2.00 (dd, ^3J = 13 Hz, ^2J = 13 Hz, 2H), 2.58 (dd, ^3J = 2 Hz, ^2J = 13 Hz, 2H), 5.30 (s, 4H), 6.09 (d, ^3J = 14 Hz, 2H), 7.2−7.5 (m, 18H), 8.23 (d, ^3J = 14 Hz, 2H). Anal. Calcd for $C_{48}H_{52}N_2ClF_6Sb$: C, 62.11, H, 5.65, N, 3.02, Found C, 62.01, H, 5.91, N, 2.90.

1·[I]. is synthesized using Method A from **1**·[Br] with [Na][I]. Single crystals suitable for X-ray diffraction analysis are obtained by slow evaporation of chloroform−toluene mixture. ^1H NMR (200.13 MHz, $CDCl_3$): δ 0.97 (s, 9H), 1.4 (m, 1H), 1.73 (s, 6H), 1.75 (s, 6H), 2.07 (dd, ^3J = 13 Hz, ^2J = 13 Hz, 2H), 2.57 (dd, ^3J = 2 Hz, ^2J = 13 Hz, 2H), 5.40 (d, ^2J = 16 Hz, 2H), 5.52 (d, ^2J = 16 Hz, 2H), 6.17 (d, ^3J = 14 Hz, 2H), 7.2−7.5 (m, 18H), 8.21 (d, ^3J = 14 Hz, 2H).

1·[$B(C_6F_5)_4$] (Method B). **1**·[Br] (50 mg, 0.06 mmol, 1 equiv) is dissolved in DCM (10 mL). Lithium tetrakis(pentafluorophenyl)borate ethyletherate (56 mg, 1 equiv) is added, and the solution is stirred 30 min at room temperature. The solution is washed with water (3 × 15 mL) and filtered trough a silica plug (washed with DCM). Then the solvents are evaporated to afford a green solid. Single crystals suitable for X-ray diffraction analysis are obtained by slow evaporation of chloroform−methanol mixture. ^1H NMR (200.13 MHz, $CDCl_3$): δ 0.89 (s, 9H), 1.35 (m, 1H), 1.69 (s, 12H), 1.91 (dd, ^3J = 13 Hz, ^2J = 13 Hz, 2H), 2.53 (dd, ^3J = 2 Hz, ^2J = 13 Hz, 2H), 5.08 (d, ^2J = 16 Hz, 2H), 5.20 (d, ^2J = 16 Hz, 2H), 5.98 (d, ^3J = 14 Hz, 2H), 7.2−7.5 (m, 18H), 8.27 (d, ^3J = 14 Hz, 2H). Anal. Calcd for $C_{72}H_{52}N_2ClBF_{20}$: C, 63.06, H, 3.82, N, 2.04, Found C, 63.42, H, 3.76, N, 2.28.

Acknowledgment. We gratefully acknowledge the reviewers for their useful comments and improvements of the quality of the manuscript. We thank the Direction Générale de l'Armement for a grant to P.A.B.. We thank Dr. S. Parola (University of Lyon) for the preparation of thin film samples; we are also grateful to the Centre de Diffractométrie Henri Longchambon (University of Lyon) for X-ray diffraction facilities. B.L.G. thanks the Pôle Scientifique de Modélisation Numérique (PSMN) at ENS Lyon for computing facilities.

Supporting Information Available: Complete ref 21. This material is available free of charge via the Internet at http://pubs.acs.org.

JA9100886

(21) Frisch, M. J.; et al. *Gaussian 03*, Revision B.04; Gaussian, Inc.: Pittsburgh, PA, 2003.
(22) Lee, C. T.; Yang, W. T.; Parr, R. G. *Phys. Rev. B* **1988**, *37*, 785–789.
(23) Becke, A. D. *J. Chem. Phys.* **1993**, *98*, 5648–5652.
(24) Cascarano, G.; Altomare, A.; Giacovazzo, C.; Guagliardi, A.; Moliterni, A. G. G.; Siliqi, D.; Burla, M. C.; Polidori, G.; Camalli, M. *Acta Crystallogr.* **1996**, *A52*, C-79.
(25) Sheldrick, G. M. *SHELX97*, Program for the refinement of crystal structures; University of Göttingen: Göttingen, Germany, 1997.